CWP-542

Increase of shear wave velocity before the 1998 eruption of Merapi volcano (Indonesia)

U. Wegler[1], B.-G. Luhr[2], R. Snieder[3] & A. Ratdomopurbo[4]
[1] *Department of Geophysics and Geology, University of Leipzig, Talstrasse 35, D-04103 Leipzig, Germany*
[2] *GeoForschungsZentrum Potsdam, Potsdam, Germany*
[3] *Department of Geophysics, Colorado School of Mines, Golden, USA*
[4] *BPPTK, volcanological Survey of Indonesia, Yogyakarta, Indonesia*

ABSTRACT
We infer temporal changes in the elastic properties of the edifice of Merapi volcano (Java, Indonesia) before its eruption in 1998 by analyzing multiply scattered elastic waves excited by a repeatable controlled seismic source. A pre-eruptive increase of shear wave velocity, which correlates well with pre-eruptive seismicity and dome-growth is revealed. The method can be used as a "pressure-gauge" for pressure changes inside of volcanoes, because increasing pressures in rocks are known to cause proportionally increasing elastic wave velocities.

Key words: time-lapse, volcano monitoring

1 INTRODUCTION

Merapi volcano, located in Java, Indonesia, is one of the most active strato volcanoes on earth. Its recent activity is characterized by repeated dome growth and (partial) dome collapse causing a permanent danger of pyroclastic flows. The 1998 eruption started on 11 July and had a second major event on 19 July. Precursors were observed in near summit tilt and in an increase of seismicity starting several weeks before the eruption (Voight et al., 2000). At the same time an active seismic experiment was carried out at Merapi volcano (Wegler and Lühr, 2001; Wegler et al., 1999). In this experiment airguns were shot in three water basins made of concrete to excite elastic waves. The main goal was to study the internal structure of the volcano with seismic methods. The seismic signals were mainly recorded along three seismic profiles, which changed their position from day to day (Wegler and Lühr, 2001). However, a few permanent seismometers are installed at Merapi volcano for monitoring purposes (Wassermann and Ohrnberger, 2001). At these permanent stations we observed the seismic signals excited by the repeatable airgun source on several different days. The combination of an active seismic experiment using a repeatable source with the onset of a volcanic eruption is a unique coincidence. It allows us to study, in detail, temporal changes in the structure of the volcano preceding the eruption. Here, we apply the concept of coda wave interferometry (Snieder et al., 2002). This method uses multiply scattered waves, which traveled through the volcanic edifice along numerous paths, to infer tiny temporal changes in the mean shear wave velocity. Using this method we are able to monitor temporal changes in relative velocity with an accuracy as small as $\delta v/v = 2 \times 10^{-4}$. Previously, such temporal changes were observed e. g. in fault zones comparing data before and after large earthquakes (Poupinet et al., 1984; Nishimura et al., 2000). At Merapi volcano earthquake multiplets were studied to infer an increase of shear wave velocity of 1.2% 8 months before the 1992 eruption (Ratdomopurbo and Poupinet 1995). Unfortunately, in that study the observation of an increasing velocity ended 4 months before the eruption. Because no more similar earthquakes occurred, further analysis was impossible. The temporal velocity changes are supposed to be caused by temporal variations of ambient stress. Laboratory experiments have shown that as a first approximation pressure changes δp cause a proportional change in the elastic wave velocities ($\delta p \sim \delta v$) (Nur, 1971; Grêt et al., 2006). Therefore, in the future, the applied method has the potential to be used as a "pressure-gauge" for monitoring pressure changes inside volcanoes. This is one of the most important parameters to predict volcanic eruptions.

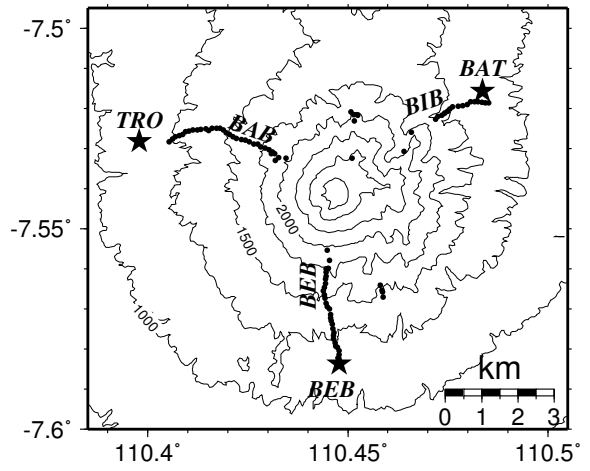

Figure 1. Topographic map of Merapi volcano with shot points (stars) and seismometer arrays (triangles).

2 OBSERVATION

The airgun shots in water basins excited elastic waves in a stable and repeatable way. This fact can be used to sample exactly the same part of the volcano at different times to monitor changes in the volcano. We use the sources and receivers shown in figure 1. The source BEB on the southern slope of Merapi volcano was shot on four different days. These shots showed sufficient signal to noise ratio at the permanent mini-array KEN with a source receiver distance of $r \approx 2.3$ km. Source BAT in the north-east was shot on three different days and signals were recorded at monitoring array GRW ($r \approx 3.6$ km). Other source receiver combinations showed insufficient signal to noise ratio for our present study. Each permanent mini-array consisted of three three-component seismometers with interstation distances of 100 - 400 m resulting in a total of 9 channels (Wassermann and Ohrnberger, 2001). At each day the airgun was shot for up to 100 times with a shot interval of 90 s. The recorded seismograms were stacked for each day. Since the observed signals mainly contain energy between 4 and 12 Hz, we applied a 2 Hz high pass filter to reduce the noise level. Additionally, we interpolated the data to decrease the sampling interval of the digital seismograms from an original value of 0.02 s to 0.004 s.

The recorded seismograms mainly consist of multiple scattered waves and their envelopes were successfully explained using the diffusion model (Wegler and Lühr, 2001; Wegler, 2005). Since P-waves are converted into S-waves more efficiently than the other way round (Aki, 1992), it is generally accepted that S-waves dominate over P-waves in the diffusion regime. The influence of surface waves, on the other hand, is more difficult to judge. Wegler and Lühr (2001) and Wegler (2005) suggested that body waves dominate in the shot seismograms recorded at Merapi, because body waves can explain the observed apparent decrease of scattering strength with increasing source receiver distance assuming a depth dependent diffusivity. In spite of the complexity of the signals we observe almost identical wave forms recorded at different days (figures 2 and 3). This indicates that source, receiver, and propagation medium did not change much between the different days. However, for some days we observe that the seismograms have almost the same wave form, but with increasing time an increasing phase shift develops between the two seismograms (figure 3, bottom). The time scale of one day appears to be stretched or compressed in comparison to another day. One might think of an unstable clock in the data recording system, but this is not the case. Firstly, for each seismometer array 6 of 9 channels were recorded by one data logger and the other 3 channels were recorded by another data logger with independent internal clocks. Nevertheless, the observed phase shifts are consistent for all 9 channels. Secondly, the observed phase shifts are as large as 0.05 s developing within a time window of 20 s. Typical phase shifts caused by the drift of instruments clocks are about 0.001 s per hour (Refraction Technology Inc., 1995) and, therefore, are four orders of magnitude smaller than the observed phase shifts. To quantify the observations shown in figure 3 we compute the cross-correlation function $R(t, T)$

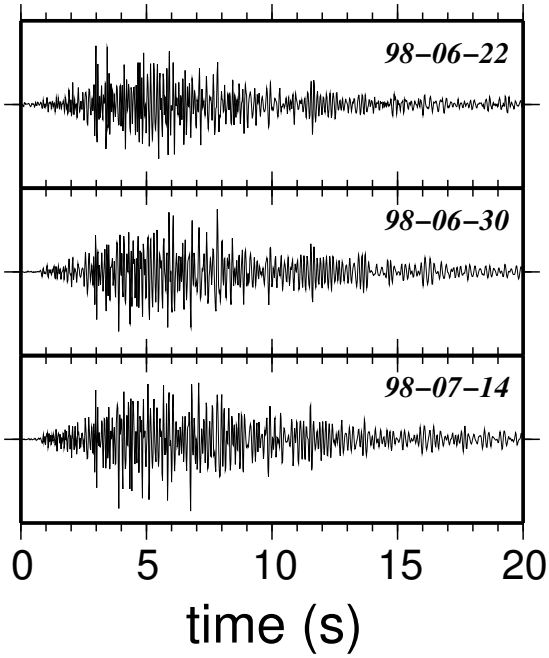

Figure 2. Vertical ground velocity at seismometer KEN0 for shots in BEB at three different days.

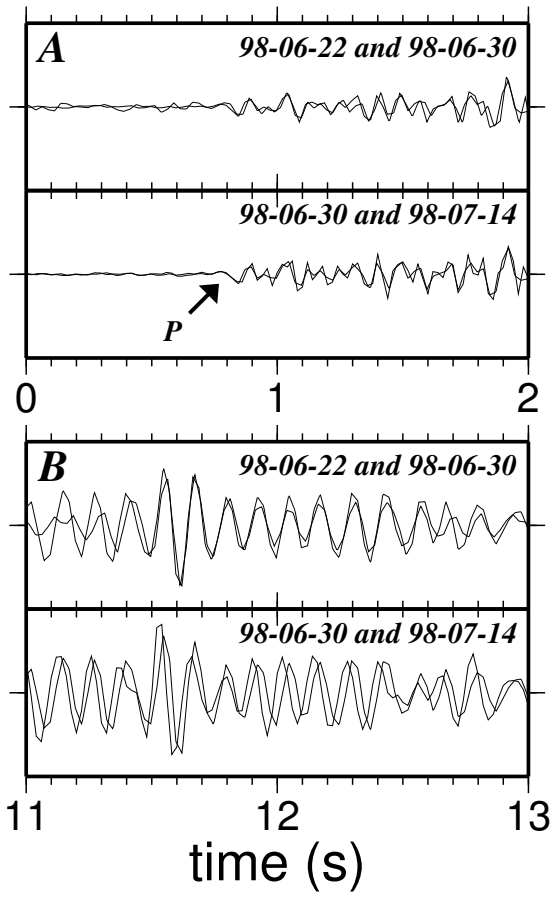

Figure 3. Vertical ground velocity at seismometer KEN0 for shots in BEB for an early time window of 0-2 s (A) and a late time window of 11-13 s after the shot time (B). The phase marked with "P" indicates the first onset of the seismogram. Each plot shows an overlay of two seismograms recorded at two different days.

of two seismograms recorded at two different days in a moving time window:

$$R(t,T) = \frac{\int_{T-\frac{\tau}{2}}^{T+\frac{\tau}{2}} u_1(t'-\frac{t}{2})\, u_2(t'+\frac{t}{2})\, dt'}{\sqrt{\int_{T-\frac{\tau}{2}}^{T+\frac{\tau}{2}} u_1^2(t')\, dt' \int_{T-\frac{\tau}{2}}^{T+\frac{\tau}{2}} u_2^2(t')\, dt'}} \qquad (1)$$

Here u_i is the measured ground velocity at day i and T is the center time of the moving time window. The cross-correlation function $R(t,T)$ depends only weakly on T and can be assumed to be constant within the time window of length τ. We used a window length of $\tau =$ 3 s, which was moved in steps of 1.5 s along the signal. t is the shift time of the cross-correlation function. In a next step we use fixed T and treat $R(t,T)$ as a function of shift time t to extract the value of its maximum, R_{max}, and the position of its maximum, δt. $R_{max}(T)$ is a measure for the similarity of two seismograms at time

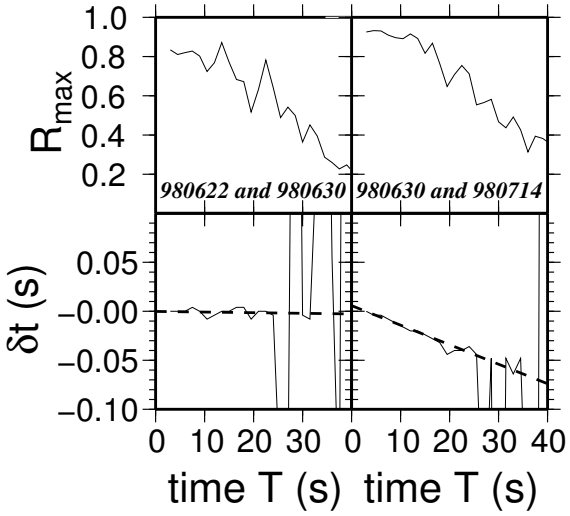

Figure 4. Top figures: Observed maximum value R_{max} of the cross-correlation coefficient as a function of time T. Bottom figures: Observed time shift δt of the maximum (continuous curve) and best fitting straight line (dashed curve). Only times with $R_{max} > 0.7$ are used to fit the data. Left hand side: vertical component of KEN0, days 98-06-22 and 98-06-30, right hand side: same component, days 98-06-30 and 98-07-14.

T and $\delta t(T)$ is a measure for the phase shift between them.

Figure 4 shows two examples for computed similarities and phase shifts. In general the similarity is high with a cross-correlation coefficient $R_{max}(T) \geq 0.7$. After a lapse time of about 20 s the amplitude of the shot signal decreases (figures 2) and after about 40 s only noise is observed with a small cross-correlation coefficient of $R_{max}(T) \leq 0.4$. The behavior of the phase shift function $\delta t(T)$ is different for the different shot pairs. For example comparing recordings of 22 June with recordings of 30 June we do not observe a phase shift (figure 4, left), whereas the comparison of 30 June and 14 July shows a linear decrease of the phase shift with time (figure 4, right). Of course, the position of the maximum is only useful, if a clear maximum exists at all. Therefore, the function $\delta t(T)$ in figure 4 should only be interpreted for times T where $R_{max}(T)$ is large ($T < 20$ s), whereas the random behavior at late times ($T > 20$ s) is meaningless.

3 INTERPRETATION

The linearly increasing phase shifts with almost constant wave forms, which were observed comparing seismograms of different days can be explained by a temporal increase of the mean velocity within the volcano in advance to the 1998 eruption. The underlying theory of coda wave interferometry (Snieder et al., 2002) assumes

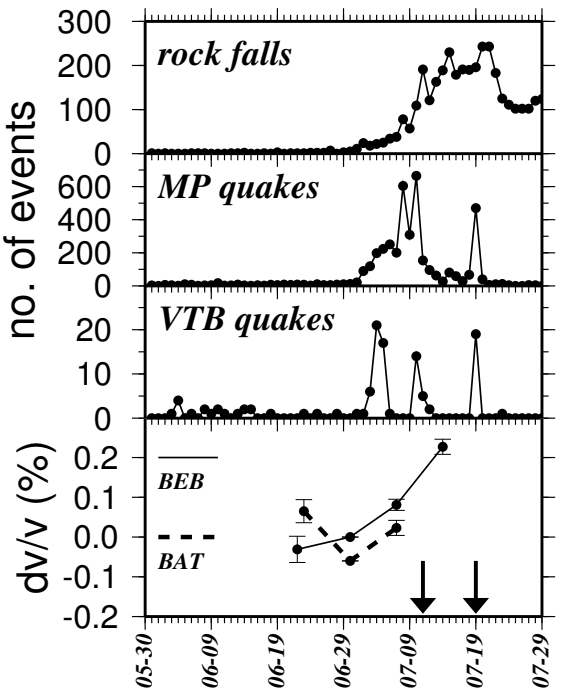

Figure 5. Top: Number of earthquakes per day for three different types of seismic signals as a function of time for the period from 30-05-1998 to 29-07-1998. Bottom: Temporal change of shear wave velocity in percent relative to shear wave velocity at 30-06-1998. The thin continuous line indicates measurement using the source in BEB and receivers in KEN. The thick dashed line indicates measurement using the source in BAT and receivers in GRW. For better visualization the absolute values of $\delta v/v$ for source BAT are shifted by -0.06. Arrows: largest events of the eruption on 11-07-1998 and 19-07-1998.

that the wave paths of multiple scattered waves remain constant, because source, receiver, and scatterer locations are identical. The phase shift is caused by the fact that waves travel the same path with a faster or slower velocity, which results for a homogeneous change on the relative velocity (Snieder, 2006):

$$\frac{\delta v}{v} = -\frac{\delta t(T)}{T} \tag{2}$$

where $\delta v/v$ is the relative change of velocity between the two days. To apply this expression to the data we fit a straight line to the observed $\delta t(T)$ curves using only those data points where the cross-correlation coefficient $R_{max}(T)$ is larger than 0.7 (figure 4). The slope of this best fitting theoretical curve gives the temporal velocity change $\delta v/v$. The results after processing data of four days at source BEB and three days at source BAT are shown in figure 5. Here, we used the statistical variations between the results for the 9 different channels (three seismometers of one mini-array times three components) to estimate a statistical error for each source receiver combination. These errors of relative velocity change are of the order of 2×10^{-4}, and are most likely caused by the finite sampling rate of 0.02 s for the digital seismograms. The data of 30 June shown in figure 5 do not have error bars, because we used the seismograms of this day as a reference. We checked that the results do not depend on the choice of the reference event. Figure 5 shows a comparison to routine seismicity measurement at Merapi (Ratdomopurbo and Poupinet, 2000) and the dates of the two major volcanic events of the 1998 eruption.

Before 2 July Merapi showed only little seismicity and the alert was at its lowest level I on a scale from I to IV. During this quiet stage the first pair of shots in BEB was on 22 June and 30 June and an almost constant or slightly increasing velocity of $\delta v/v = (0.03 \pm 0.03)$ % was observed. For almost the same period (23 - 30 June) shots at source BAT indicate a velocity decrease of (0.13 ± 0.03) %. Then, according to our interpretation, the pressure inside the volcano increased. This stress change inside the volcano caused the occurrence of shallow volcano tectonic earthquakes (VT-B in figure 5). Additionally, dome growth accelerated, which in turn also caused an increasing number of rock falls and so-called MP-quakes. The onset of this significant seismicity caused the Volcanological Survey of Indonesia to set the alert to level II on 2 July. Further increasing seismicity and near summit tilt data caused another increase of the alert level to III on 8 July (Voight, et al., 2000). During this pre-eruptive stage the third shot day for both sources was at 7 July, five days after seismicity started and four days before the first eruption. For this period (30 June - 7 July) we observe an increase of velocity of $\delta v/v = (0.08 \pm 0.01)$ % in BEB and an identical increase of $\delta v/v = (0.08 \pm 0.02)$ % in BAT.

We propose that this velocity increase can be assumed to be directly proportional to the increasing pressure inside the volcano. Such dependency of rock velocities on stress was proven in many laboratory experiments (Nur, 1971; Gret et al., 2006). The 1998 eruption started on 11 July with 36 pyroclastic flows having a maximum runout of 5.5 km. A second major event of this eruption occurred on 19 July with 25 pyroclastic flows with a maximum length of 5.5 km (Voight, 2000). A fourth shot only exists for source point BEB on 14 July, three days after the onset of the eruption and five days before the second major volcanic event. Relative to 30 June the velocity increased in total by $\delta v/v = (0.23 \pm 0.02)$ %, which indicates that the pressure inside the volcano was not reduced by the first eruption, but was still increasing, probably until the second event on 19 July.

4 DISCUSSION

Within our simple model we cannot explain the decrease of velocity, which was observed for source BAT

during the quite period (23 - 30 June). Clearly, there is no simple model for this observation, because the volcano shows different behavior on its north-eastern slope compared to its southern slope. However, the two different shot-receiver pairs sample different regions of the volcanic edifice. Pacheco and Snieder (2005) studied the sensitivity of diffusive wave to localized velocity changes. These authors reported that coda wave interferometry is expecially sensitive to medium changes in an ellipse with foci at the source and receiver location. Therefore, one might think of two possible explanations for the differences between the observations at BEB and BAT. First, in reality the pressure source inside the volcano has a certain position (e. g. spherical or dike source,) whereas in our model we assumed a spatially constant relative velocity shift caused by a spatially constant pressure change. Second, spatial variations in the structure of the volcano exist. The north-eastern slopes of Merapi are deposits of so-called "old Merapi", whereas in the south-west the much younger and unconsolidated deposits of so-called "new Merapi" dominate (Newhall et al., 2000). These structural differences result in spatially dependent elastic properties of the volcanic edifice, which are neglected in our approach. Both effects, a spatially dependent input pressure as well as spatially dependent elastic properties of the volcano might explain the observed differences between measurements on the southern and on the north-eastern slope. To understand such spatial differences much more source receiver combinations are necessary than were available in our experiment. Additionally, much longer time periods using shots on many different days should be studied to analyze the influence of other parameters like meteorology which might also cause temporal variations in seismic velocity.

ACKNOWLEDGMENTS

The seismic field experiment was financially supported by the Deutsche Forschungsgemeinschaft (DFG) under grant no. Zs 4/16-1,2. We thank BPPTK Yogyakarta and the students of Gadjah Mada University, Yogyakarta, for their logistical support during the field work. The critical reviews of C. Bean and T. Nishimura helped to improve this article.

REFERENCES

Aki, K., Scattering conversions P to S versus S to P, *Bull. Seismol. Soc. Am.*, *82*(4), 1969–1972, 1992.

Grêt, A., R. Snieder, and J. Scales, Time-lapse monitoring of rock properties with coda wave interferometry, *J. Geophys. Res.*, in press, 2006.

Newhall, C. G., et al., 10,000 years of explosove eruptions of Merapi volcano, central Java: archaeological and modern implications, *J. Volcanol. Geotherm. Res.*, *100*, 9–50, 2000.

Nishimura, T., N. Uchida, H. Sato, M. Ohtake, S. Tanaka, and H. Hamaguchi, Temporal changes of the crustal structure associated with the M6.1 earthquake on September 3, 1998 and the volcanic activity of mount Iwate, Japan, *Geophys. Res. Lett.*, *27*(2), 269–272, 2000.

Nur, A., Effects of stress on velocity anisotropy in rocks with cracks, *J. Geophys. Res.*, *76*(8), 2022–2034, 1971.

Pacheco, C., and R. Snieder, Time-lapse travel time change of multiply scattered acoustic waves, *J. Acoust. Soc. Am.*, *118*(3), 1300–1310, 2005.

Poupinet, G., W. L. Ellsworth, and J. Frechet, Monitoring velocity variations in the crust using earthquake doublets: an application to the Calaveras fault, California, *J. Geophys. Res.*, *89*(B7), 5719–5731, 1984.

Ratdomopurbo, A., and G. Poupinet, Monitoring a temporal change of seismic velocity in a volcano: application to the 1992 eruption of Mt. Merapi (Indonesia), *Geophys. Res. Lett.*, *22*(7), 775–778, 1995.

Ratdomopurbo, A., and G. Poupinet, An overview of the seismicity of Merapi volcano (Java,Indonesia), 1983-1994, *J. Volcanol. Geotherm. Res.*, *100*, 193–214, 2000.

Refraction Technology Inc., *RefTek Operations Reference Manual*, 2626 Lombardy Lane, Suite 105, Dallas, TX 75220, 1995.

Snieder, R., The theory of coda wave interferometry, *Pure Appl. Geophys.*, in press, 2006.

Snieder, R., A. Grêt, H. Douma, and J. Scales, Coda wave interferometry for estimating nonlinear behaviour in seismic velocity, *Science*, *295*, 2253–2255, 2002.

Voight, B., et al., Deformation and seismic precursors to dome-collapse and fountain-collapse nuées ardentes at Merapi Volcano, Java, Indonesia, 1994-1998, *J. Volcanol. Geotherm. Res.*, *100*, 261–287, 2000.

Wassermann, J., and M. Ohrnberger, Automatic hypocenter determination of volcano induced transients based on wavefield coherence - an application to the 1998 eruption of Mt. Merapi, indonesia, *J. Volcanol. Geotherm. Res.*, *110*, 57–77, 2001.

Wegler, U., Diffusion of seismic waves in layered media: Boundary conditions and analytical solutions, *Geophys. J. Int.*, *163*(3), 1123–1135, 2005.

Wegler, U., and B.-G. Lühr, Scattering behaviour at Merapi volcano (Java) revealed from an active seismic experiment, *Geophys. J. Int.*, *145*, 579–592, 2001.

Wegler, U., B.-G. Lühr, and A. Ratdomopurbo, A repeatable seismic source for tomography at volcanoes, *Annali di Geofisica*, *42*(3), 565–571, 1999.